Title

VPS32, a member of the ESCRT complex, modulates adherence to host cells in the parasite Trichomonas vaginalis by affecting biogenesis and cargo sorting of released extracellular vesicles.

Journal

Cellular and Molecular Life Sciences, 79(1)

Authors

Salas, Nehuén
Coceres, Veronica
Melo, Tuanne
et al.

Publication Date

2021-12-24

DOI

10.1007/s00018-021-04083-3

Peer reviewed

Cellular and Molecular Life Sciences (2022) 79:11
https://doi.org/10.1007/s00018-021-04083-3

ORIGINAL ARTICLE

VPS32, a member of the ESCRT complex, modulates adherence to host cells in the parasite *Trichomonas vaginalis* by affecting biogenesis and cargo sorting of released extracellular vesicles

Nehuén Salas[1] · Veronica M. Coceres[1] · Tuanne dos Santos Melo[2] · Antonio Pereira-Neves[2] · Vanina G. Maguire[1] · Tania M. Rodriguez[1] · Bruna Sabatke[3] · Marcel I. Ramirez[3] · Jihui Sha[4] · James A. Wohlschlegel[4] · Natalia de Miguel[1]

Received: 9 July 2021 / Revised: 6 December 2021 / Accepted: 8 December 2021 / Published online: 24 December 2021

Abstract

Trichomonas vaginalis is a common sexually transmitted extracellular parasite that adheres to epithelial cells in the human urogenital tract. Extracellular vesicles (EVs) have been described as important players in the pathogenesis of this parasite as they deliver proteins and RNA into host cells and modulate parasite adherence. EVs are heterogeneous membrane vesicles released from virtually all cell types that collectively represent a new dimension of intercellular communication. The Endosomal Sorting Complex Required for Transport (ESCRT) machinery contributes to several key mechanisms in which it reshapes membranes. Based on this, some components of the ESCRT have been implicated in EVs biogenesis in other cells. Here, we demonstrated that VPS32, a member of ESCRTIII complex, contribute to the biogenesis and cargo sorting of extracellular vesicles in the parasite *T. vaginalis.* Moreover, we observe that parasites overexpressing VPS32 have a striking increase in adherence to host cells compared to control parasites; demonstrating a key role for this protein in mediating host: parasite interactions. These results provide valuable information on the molecular mechanisms involved in extracellular vesicles biogenesis, cargo-sorting, and parasite pathogenesis.

Keywords Extracellular vesicles · ESCRTIII complex · VPS32 · *Trichomonas vaginalis*

Introduction

Trichomonas vaginalis is a flagellated, unicellular, microaerophilic protozoan pathogen of the human urogenital tract that causes a highly prevalent sexually transmitted infection (STI) [1]. Although infections are generally mild or asymptomatic, disease manifestation might include discomfort in the urogenital area as a consequence of vaginitis or urethritis as well as preterm delivery and premature rupture of membranes if acquired during pregnancy [2]. Furthermore, serious adverse consequences include increased risk of both human immunodeficiency virus (HIV) transmission and acquisition [3, 4] and increased risk of malignant cervical and prostate cancers [5, 6]. As an exclusively extracellular pathogen, *T. vaginalis* attachment to host cells is crucial for host colonization and infection establishment. Recently, new factors in this process have been identified; including parasites secreted vesicles as well as surface and secreted proteins [7, 8]. As a result, the study of extracellular vesicles (EVs) has become an active endeavor in the study of pathogenesis in this parasite.

EVs are a heterogeneous group of cell-derived membranous structures that are classified based on their mechanism of biogenesis or size into three major categories: exosomes, microvesicles (MVs), and apoptotic bodies. So far, the release of exosomes and MVs have been described in *T. vaginalis* [9, 10]. Interestingly, the formation of both types of EVs increase when *T. vaginalis* is expose to host cells,

✉ Natalia de Miguel
ndemiguel@intech.gov.ar

[1] Laboratorio de Parásitos Anaerobios, Instituto Tecnológico Chascomús (INTECH), CONICET-UNSAM, Intendente Marino Km 8.2, B7130IWA Chascomús, Buenos Aires, Argentina

[2] Departamento de Microbiologia, Instituto Aggeu Magalhães, Fiocruz, Recife, Pernambuco, Brazil

[3] Laboratorio de Biologia Molecular e Sistémica de Tripanossomatideos, Instituto Carlos Chagas, Fiocruz Curitiba, Parana, Brazil

[4] Department of Biological Chemistry, University of California, Los Angeles, CA 90095-1489, USA

indicating that might have a role in host: parasite interaction and/or cell communication [9, 10]. Interestingly, exosomes contain strain-specific content and that they have effects on both host and parasites [9]. Exosomes, with size range from 30 to 150 nm in diameter, are secreted upon fusion of multivesicular bodies (MVBs) with the plasma membrane and release of contained intraluminal vesicles (ILVs). Ectosomes or MVs, ranging from 100 to 1000 nm in diameter, are release into the extracellular space by the direct budding and extrusion of the plasma membrane [11]. Even though there are differences in the biogenesis process between exosomes and MVs, studies in mammalian cells demonstrated that both routes share some sorting machineries for their generation, such as Tetraspanin and/or 'Endosomal Sorting Complex Required for Transport' (ESCRT) proteins [11, 12]. The ESCRT complexes comprise an ancient system, conserved from yeast to mammals, for membrane remodeling and scission of approximately 20 proteins that assemble into 4 complexes (ESCRT-0, -I, -II and -III) [11, 13–15]. Specifically for exosome formation, a critical aspect of the process is the accumulation and processing of ubiquitinated proteins that are transferred by the ESCRT machinery from the plasma membrane and endosomes to the budding ILVs [16]. The four ESCRT complexes, each comprising several subunits, play distinct roles: ESCRT-0 binds and sequesters the ubiquitinated proteins; ESCRT- I, in concert with ESCRT-II, initiates local budding of the endosomal membrane; and ESCRT-III participates in protein deubiquitination as well as provide the energetic force that drives membrane scission and detachment of vesicles into the endosome lumen [16, 17]. Particularly, the ESCRT-III component protein SNF7 forms the oligomeric assemblies that promote vesicle budding. Initially, the ESCRT machinery was considered important only for the formation of ILVs inside the MVBs. However, ESCRTs play important roles in other processes specific to the plasma membrane involving sorting, budding, and fission, such as cytokinesis and virus budding [18–20]. In this context, recent evidence demonstrates that some ESCRT subunits participate in the assembly and budding of MVs [16]. Specifically, ESCRT-III has been shown to be critical for the pinching off and release of MVs [21]. Several models have been proposed to interpret the interaction of ESCRT-III with the cytoplasmic surface of ILVs and MVs domains: driving membrane deformation and cargo sorting [22], polymer driven membrane buckling [23], and dome-based membrane scission [24]. Although the role of ESCRT-III-dependent EVs formation have been described in mammalian systems, the involvement of these proteins in targeting eukaryotic microbial EVs only recently has been proposed [25]. In *T. vaginalis*, proteomic analyses of isolated exosomes and MVs identified a component of the ESCRT machinery named ESCRT-III subunit vacuolar protein sorting-associated protein 32 (VPS32, also known SNF7) [9, 10]. This protein has also been associated with regulation of *Tritrichomonas foetus* cell division [26]. In this context and as a step toward further understanding the role of ESCRT complex in biogenesis of EVs in protozoan parasites, here, we have examined the role of VPS32 in EVs formation in *T. vaginalis*. Interestingly, our data indicate a key role for this protein in the biogenesis and cargo sorting of EVs. Importantly, we also demonstrate that VPS32 plays a central role in regulation of parasite attachment to prostate cells and contribute to *T. vaginalis* pathogenesis. Taken together, our data indicate that VPS32 activity is important for generating extracellular vesicles, thereby generally implicating the ESCRT machinery in EV biogenesis and shedding light on the understanding of *T. vaginalis* pathogenesis.

Material and methods

Parasites, cell cultures and media

Trichomonas vaginalis strain G3 (ATCC PRA-98; Kent, UK) was cultured in TYM medium supplemented with 10% horse serum and 10 U/ml penicillin [27]. Parasites were grown at 37 °C and passaged daily. The human NHPrE1 cells were kindly provided by Dr. Simon Hayward (North-Shore University, USA) [28]. NHPrE1 cells were grown in 50/50 Dulbecco's modified Eagle medium (DMEM)/F12 containing 5% fetal bovine serum (FBS; Atlanta Biologicals, Lawrenceville, GA, http://www.atlantabio.com), 1% insulin-transferrin-selenium-X (ITS) (Gibco, Grand Island, NY, http://www.invitrogen.com), 0.4% bovine pituitary extract (BPE; Hammond Cell Tech, Windsor, CA, http://www.hammondcelltech. com), and 1:1,000 10 ng/ml epidermal growth factor (EGF; Sigma-Aldrich, St. Louis, MO, http://www.sigmaaldrich.com) with 10 U/ml penicillin and cultured at 37 °C/5% CO_2 as previously described [28].

Plasmid construction and exogenous expression in *T. vaginalis*

The VPS32 (TVAG_459530) full length construct gene was PCR-amplified using the following primer pairs: forward (5′-3′ AAACATATGATGAGCTGGTTATGGGGTAAGAAG AAG) and reverse (5′- 3′ TTTGGTACCATCATGGCTCAG TTCGGTGGTATC); containing NdeI and KpnI restriction sites, respectively. PCR fragments were then cloned into the master-Neo-$(HA)_2$ plasmid [29]. Electroporation of *T. vaginalis* strain G3 was carried out as described previously [29] with 50 µg of circular plasmid DNA. Parasites were transfected in parallel with an empty plasmid (EpNEO) to be used as control. Transfectants were selected with 100 µg/ml G418 (Sigma).

Transmission Electron Microscopy (TEM)

Routine negative staining

EVs samples were fixed in 2.5% glutaraldehyde in 0.1 M cacodylate buffer, pH 7.2, settled onto glow discharge carbon film nickel grids for 5 min at room temperature, and negatively stained with 1% aurothioglucose (UPS Reference Standard) in water for 5 s. The grids were then air-dried and observed with a FEI Tecnai G2 Spirit transmission electron microscope, operating at 120 kV. The images were randomly acquired with a CCD camera system (MegaView G2, Olympus, Germany).

Immunogold

For immunogold labelling, three complementary procedures were assessed as described below. As negative control, the primary antibodies were omitted, and the samples were incubated with the gold-labelled goat anti-mouse antibody only. No labelling was observed under this condition.

Postembed labeling

Parasites were fixed in 4% paraformaldehyde, 0.5% glutaraldehyde, 0.1% picric acid in 0.1 M cacodylate buffer (pH 7.2) overnight at 4 °C. Afterwards, the cells were washed in PBS, dehydrated in ethanol, and embedded in Unicryl resin (Electron Microscopy Sciences, USA). Ultra-thin sections were harvested on 300 mesh nickel grids and quenched in 50 mM ammonium chloride, 3% and 1% BSA, and 0.2% Tween-20 in PBS (pH 8.0). Next the grids were incubated with anti-HA tag antibody (Invitrogen, 5B1D10), 10 × diluted in 1% BSA in PBS for 3 h at room temperature. The grids were washed with 1% BSA in PBS and labelled for 60 min with 10 nm gold-labelled goat anti-mouse IgG (BB International, UK), 100 × diluted in 1% BSA in PBS. After several washes in PBS and water, the grids were stained with uranyl acetate and lead citrate and observed as described above.

Preembed labeling

Parasites were prefixed in 4% paraformaldehyde, 0.5% glutaraldehyde in 0.1 M cacodylate buffer (pH 7.2) for 20 min at room temperature. After washes in PBS, the cells were quenched and incubated with anti-HA and 10 nm gold-labelled anti-mouse antibodies as mentioned above. After several washes in PBS and distilled water, parasites were re-fixed in 2.5% glutaraldehyde in 0.1 M cacodylate buffer (pH 7.2) for 2 h at room temperature, post-fixed for 30 min in 1% OsO4, dehydrated in acetone and embedded in Epon Polybed 812. Ultra-thin sections were harvested, stained with uranyl acetate and lead citrate and observed as mentioned above.

Negative stain labeling

EVs samples were settled onto glow-discharge carbon coated nickel grids for 10 min at room temperature, followed by fixation with 4% paraformaldehyde, 0.5% glutaraldehyde in 0.1 M cacodylate buffer (pH 7.2) for 1 h at room temperature. After washes in PBS, the grids were quenched and incubated with anti-HA and 10 nm gold-labelled anti-mouse antibodies as described above. Samples were washed with water, negatively stained with 1% aurothioglucose and observed as mentioned above.

Isolation of *T. vaginalis* vesicles

As recommended, the exosome and microvesicles (MVs) nomenclature will be used throughout the text for the two individual classes of vesicle and the term EVs when both populations are taken together [30]. EVs isolation will be performed using wild type or TvEpNEO and TvVPS32 transfected *T. vaginalis* (10^6 cells/ml). To this end, 5×10^8 parasites were washed and incubated for 4 h at 37 °C in 500 ml of TYM medium without serum to stimulate EVs release. Then, conditioned medium was harvested and centrifuged (3000 rpm for 10 min) to remove cell debris. The media were filtered through 0.8 µm filter and the sample was pelleted by centrifugation at 100,000 × g for 90 min to obtain an EVs enriched fraction (a mixture of MVs and exosomes). The pellet was resuspended in 200 µl cold PBS + 1X cOmplete™ ULTRA Tablets, Mini, EASYpack Protease Inhibitor Cocktail (Sigma).

SDS-PAGE and Western Blot

EVs lysates were analyzed by sodium dodecyl sulfate–polyacrylamide gel electrophoresis (SDS-PAGE). For comparison, equal volume of samples was electrophoretically separated on 12% SDS-PAGE gels and electrotransferred onto PVDF blotting membranes (GE Healthcare, Life Science). The membranes were blocked in 5% (w/v) skim milk powder in Tris-buffered saline with 0.05% (v/v) Tween 20 (TBST) for 1 h at RT and then probed with rabbit anti-TCTP (1:500), rabbit anti–TSP1 (1:500), rabbit anti-MIF (1:500) and rabbit anti–Hmp33 (1:500). Labeling was visualized with secondary antibodies anti-rabbit-AP (1:10,000) (Sigma) using the NBT/BCIP system (Roche).

Total protein quantification

Total protein concentration was determined colorimetrically (Bradford Reagent, Sigma-Aldrich). The standard curve was prepared using Bovine Serum Albumin (Promega). Absorbance was measured at 595 nm with a spectrophotometer.

EVs quantification

Nanoparticle tracking analysis (NTA, Nanosight, Malvern, U.K.) was used to quantified EVs released by VPS32 and EpNEO transfected parasites. Each sample was diluted 1:100 in PBS and subjected to a NS300 Nanosight. Each sample was analyzed in triplicate using 60 s videos at 10 frames per second at room temperature, with the following parameters: camera shutter—1492, camera gain—512, detection threshold—10.

EVs labeling

T. vaginalis was grown to a density of 1×10^6 cells/ml in TYM media and EVs were isolated as described. EVs were subjected to PKH67 Green Fluorescent Cell Linker for General Cell Membrane Labeling (Sigma-Aldrich) according to the manufacture's recommendations. Briefly, 10 µg of EVs were labeled with 4 µl of PKH67 for 5 min at room temperature in 1 ml of Diluent C. As a control, the same volume of PBS was labeled with PKH67. To remove unincorporated dye, the samples were subsequently passed through 10 kDa Amicon Ultra Centrifugal Filters (Milipore)**.**

Binding of EVs to prostate cells

To carry out the binding step, 10 µg of the PKH67 labelled EVs or the same volume of the PKH67-PBS control were added to confluent NHPrE1 cells in a 24-well plate and incubated for 3 h at 37 °C. When stated, the incubation was also performed at 4 °C. The cells were washed twice with PBS and fixed using 4% paraformaldehyde for 15 min. The nuclei were stained by DAPI fluorescent stain (Sigma-Aldrich), according to the manufacturer's protocol and examined using a Zeiss Axio Observer 7 (Zeiss) inverted fluorescence microscope. All images were acquired at the same exposure time, brightness and contrast.

The binding of the EVs to the prostate cells was also analyzed by a BD FACSCalibur flow cytometer (BD Biosciences). Briefly, 1×10^6 NHPrE1 cells were incubated with 10 µg of labeled EVs for 45 min, washed and used for flow cytometry analysis. NHPrE1 cells were used as untargeted cell control. Additionally, a control tube (dye in PBS) was included to ensure lack of fluorescence in the absence of EVs. The data were analyzed using FlowJo software (FlowJo, LLC, Ashland, OR, USA).

Attachment assay

Attachment of parasites to NHPrE1 cells was performed as described [9]. Briefly, Cell Tracker Blue CMAC (Invitrogen) labeled parasites were added to confluent monolayer of host cells (1:3 parasite:host cell ratio) for 30 min. Coverslips were subsequently rinsed in PBS to remove unattached parasites, fixed with 4% formaldehyde (Polysciences, Inc), and mounted on slides with Fluoromont Aqueous Mounting Medium (Sigma). Fluorescent parasites attached to host cells were visualized using a Zeiss Axio Observer 7 (Zeiss) microscope and quantified using ImageJ.

Proteomic mass spectrometry analysis

EVs' pellet was re-suspended in a minimal volume of digestion buffer (100 mM Tris–HCl, pH 8, 8 M urea). Re-suspended proteins were reduced and alkylated by the sequential addition of 5 mM tris(2-carboxyethyl) phosphine and 10 mM iodoacetamide as described previously. The samples were then digested by Lys-C (Princeton Separations) and trypsin proteases (Promega) [31]. First, Lys-C protease [~ 1:50 (w/w) ratio of enzyme:substrate] was added to each sample and incubated for 4 h at 37 °C with gentle shaking. The digests were then diluted to 2 M urea by the addition of digestion buffer lacking urea, and trypsin was added to a final enzyme:substrate ratio of 1:20 (w/w) and incubated for 8 h at 37 °C with gentle shaking. Digests were stopped by the addition of formic acid to a final concentration of 5%. Supernatants were carefully removed from the resin and analyzed further by proteomics mass spectrometry. Digested samples were then analyzed using a LC–MS/MS platform as described previously [32, 33]. Briefly, digested samples were loaded onto a fused silica capillary column with a 5-µm electrospray tip and packed in house with 18 cm of Luna C18 3 µM particles (Phenomenex). The column was then placed in line with a Q-exactive mass spectrometer (Thermo Fisher), and peptides were fractionated using a gradient of increasing acetonitrile. Peptides were eluted directly into the mass spectrometer, where MS/MS spectra were collected. The data-dependent spectral acquisition strategy consisted of a repeating cycle of one full MS spectrum (resolution = 70,000) followed by MS/MS of the 12 most intense precursor ions from the full MS scan (resolution = 17,500) [34]. Raw data and spectra analyses were performed using the MaxQuant software [35]. For protein identification a search against a fasta protein database was done consisting of all predicted open reading frames downloaded from TrichDB on May 20, 2021 [36] concatenated to a decoy database in which the amino acid sequence of each entry was reversed. The following searching parameters were used: (1) precursor ion tolerance was 20 ppm; (2) fragment ion tolerance was 20 ppm; (3) cysteine carbamidomethylation

was considered as a static modification; (4) peptides must be fully tryptic; and (5) no consideration was made for missed cleavages. False positive rates for peptide identifications were estimated using a decoy database approach and then filtered using the DTASelect algorithm [37–39]. Proteins identified by at least two fully tryptic unique peptides, each with a false positive rate of less than 5%, were considered to be present in the sample. Three different sets of samples were independently analyzed. Proteins present in the EVs' fraction were identified using BLAST tool (Basic Local Alignment Search Tool) and classified using the GO term enrichment according to PANTHER Classification System [40].

Graphics and statistical analyses

Specific statistical considerations and the tests used are described separately for each subsection. GraphPad Prism for Windows version 8.00 and RStudio version 4.0.5 (http://www.R-project.org) were used for graphics. Data are given as mean ± standard deviation (SD). Significance was established at $p < 0.05$. For statistical analyses, InfoStat software version 2020e was used.

Results

VPS32 is localized in secreted EVs

We have previously demonstrated that *T. vaginalis* secretes exosomes and MVs [9, 10]. Additionally, VPS32 was previously detected in the exosomes and MVs proteomes [9, 10]. To determine whether VPS32 is localized in compartments related to EVs formation, we cloned the gene in our standard *T. vaginalis* expression vector [29], under the control of a strong *T. vaginalis* promoter and fused with two C-terminal hemagglutinin (HA) tags. The construct was then introduced into a low adherent *T. vaginalis* strain (G3) by transfection, and parasites were selected with G418 as previously described [29]. Using an immunoelectron microscopy assay with an anti-HA antibody, exogenously overexpressed VPS32 was found to localize to intraluminal vesicles (ILVs) inside the MVBs (Fig. 1a) as well as MVs that protrude from the cell surface (Fig. 1b). Additionally, it is also found in EVs being endocytosed or exocytosed in or out of the cell, respectively (Fig. 1c). To demonstrate that VPS32 is localized in secreted EVs, we used a modified version of the exosome isolation protocol [9] to isolate a population

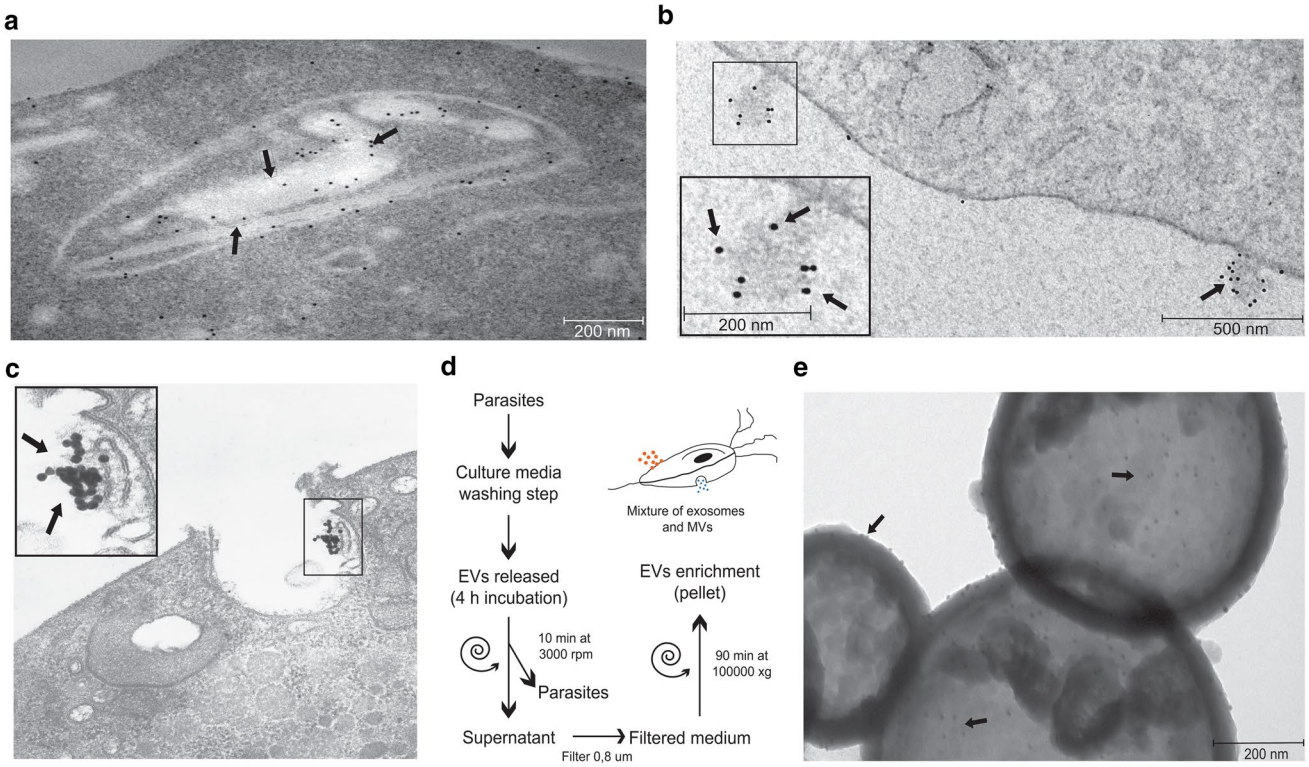

Fig. 1 Localization of VPS32 protein. **a–c** Electron micrographs of ultrathin cryosections of TvVPS32-HA transfected parasites immunogold-labelled with anti-HA antibodies demonstrate that VPS32 is localized in ILVs inside MVBs (**a**), microvesicles (MVs) protruding from the cell surface (**b**) and EVs being endocytosed or exocytosed in or out of the cell (**c**). **d** EVs isolation protocol. **e** VPS32 localization in isolated EVs analyzed by immunoelectron-microscopy using an anti-HA antibody. Arrows indicate colloidal gold particles

of vesicles, smaller than 800 nm, from parasites transfected with VPS32 (Fig. 1d). To this end, parasites were incubated for 4 h in serum-free media to allow EV release. After incubation, the samples were centrifuged to remove parasites and the supernatant was filtered through a membrane with a nominal diameter pore of 800 nm to avoid cell debris contamination. Particles with sizes smaller than 800 nm, containing a mixture of exosomes and MVs, were centrifuged at 100.000 × g for 90 min to concentrate (Fig. 1d). Examination of the preparations using an immunoelectron microscopy assay with an anti-HA antibody revealed that VPS32 is present in the isolated EVs fraction (Fig. 1e). Based on these results, we hypothesized that VPS32 might be involved in regulation of EVs formation.

VPS32 modulates EV secretion

Using classical purification and detection procedures, our results indicates that VPS32 overexpression increase the secretion of EVs in transfected parasites. Specifically, EVs were isolated by differential ultracentrifugation of the supernatant of equal numbers of parasites transfected with VPS32 (TvVPS32) or an empty plasmid (TvEpNEO) and the sample obtained after a final 100,000 × g ultracentrifugation was analyzed by complementary techniques (EM, NTA, protein quantification and western blotting). As observed in Fig. 2a, an increased amount of EVs secreted by TvVPS32 is observed by electron microscopy when compared to TvEpNEO parasites (Fig. 2a). The amount of secreted EVs was indirectly determined by measuring the total amount of protein by Bradford assay (Fig. 2b) or SDS-PAGE (Fig. 2c) in the isolated EVs samples. Consistent with our TEM, a clear increase in the amount of proteins released by TvVPS32 was detected when compared to TvEpNEO control cells. To evaluate if the observed differences in proteins abundance among samples are due to a different amount of secreted EVs, western blot analysis detecting proteins previously found in the exosome and MVs proteomes was performed [9, 10]. To this end, an integral membrane protein (TvTSP1) as well as two cytosolic proteins (TvMIF and TvTCTP) were selected. Consistent with previous findings, an increased signal of protein localized in EVs (TvTSP1, TvTCTP, TvMIF), but not in the whole cell lysate, was observed by western blotting when EVs are isolated from the supernatant of the same number of TvVPS32 or TvEpNEO parasites (Fig. 2d), which suggests an increase in total EV secretion by VPS32-overexpressing cells. Furthermore, the number and size of released EVs was analyzed by nanoparticle tracking analysis (NTA) demonstrating that ~ 2,threefold increase in the total number of particles was obtained from TvVPS32 compared to TvEpNEO control (Fig. 2e). To evaluate the origin of the EVs induced in the TvVPS32 cells, an alternative differential centrifugation-based protocol has been performed (Fig. 3a) and the samples obtained after a 10.000 × g and 100.000 × g centrifugation has been analyzed by NTA (Fig. 3b). The results demonstrated that the number of EVs obtained after a 10.000 × g centrifugation is higher in TvVPS32 transfected cells than EpNEO parasites. As these samples are enriched in larger vesicles (Fig. 3b), these results are indicating that TvVPS32 might have a role in MVs release. However, it was not possible to analyze the role of TvVPS32 in small EVs release by NTA as the sample obtained at 100.000 × g also contains a great amount of large EVs. Further analyses are needed to improve the small EVs isolation protocol. Alternatively, when the size of secreted vesicles was analyzed by electron microscopy, EVs released by TvVPS32 cells are similar in size and morphology to EVs produced by TvEpNEO control parasites (Fig. 3c), suggesting that both types of EVs are being affected. In summary, these complementary results show that overexpressing VPS32 might increase the amount of exosomes and MVs released in the cell culture supernatant, indicating a role for this protein in EVs biogenesis.

VPS32 contributes to increased host cell binding

As a parasite that does not invade host cells, attachment to urogenital epithelial cells is a critical step for *T. vaginalis* pathogenesis [7]. Therefore, understanding the molecular mechanisms of how *T. vaginalis* attaches to host cells is key to understanding how the parasite establishes infection. However, previous attempts to characterize specific parasite proteins involved in host binding suggested that the process is mediated by multiple factors, and many are yet to be defined [41, 42]. As EVs have been shown to be important for host binding [9] and we demonstrated that VPS32 regulates EVs biogenesis, we decided to evaluate whether VPS32 might have a role in modulating parasite adherence. To this end, we compared the abilities of VPS32-overexpressing parasites to bind host NHPrE1 prostate cells. Remarkably, we found that overexpression of VPS32 drastically increases the attachment to host cells ~ 33-fold compared to the TvEpNEO control (Fig. 4a and b).

VPS32-EVs have higher uptake by host cells

To address whether the observed effect in parasite attachment is modulated by the EVs released, NHPrE1 cells were cultured in plates, pre-incubated with increasing amounts of EVs isolated from TvVPS32 or TvEpNEO and examined using the in vitro parasite attachment assay (Fig. 4c). As previously demonstrated [9], pre-incubation with EVs isolated from TvEpNEO and/or TvVPS32 increase the attachment of a poorly adherent parasite strain G3 (Fig. 4d). This finding supports a role for *T. vaginalis*-derived EVs in regulation of parasite attachment. Interestingly, a stronger effect in

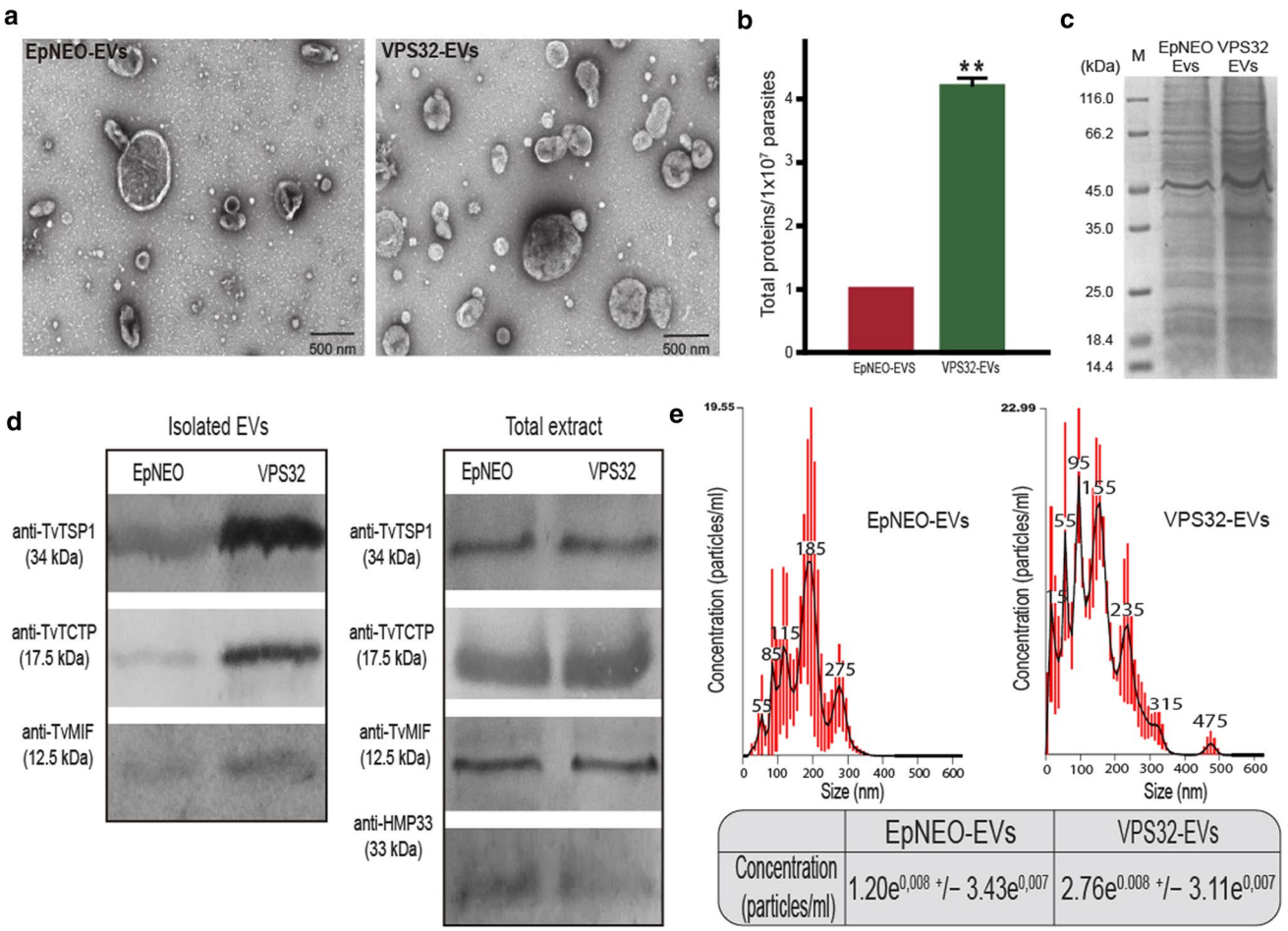

Fig. 2 Large-scale isolation and characterization of EVs secreted by TvVPS32 and TvEpNEO parasites. **a** EVs isolated from TvVPS32 (VPS32-EVs) and TvEpNEO (EpNEO-EVs) cell culture supernatants were negatively stained and analyzed using transmission electron microscopy. Scale bar, 500 nm. **b** The total amounts of proteins in the EVs pellet isolated from large-scale cultures of TvVPS32 and TvEpNEO control parasites were quantified by Bradford Reagent (Sigma-Aldrich) and are presented as the values per 10^7 secreting parasites. Data are the mean ± SD. from three independent experiments ($p < 0.01$). **c** Characterization of EVs proteins by SDS-PAGE. Isolated EVs secreted by equal numbers of TvVPS32 or TvEpNEO parasites were analyzed by SDS-PAGE. Same volume of samples was loaded on the gel. **d** Characterization of EVs proteins by immunoblotting. Whole cell lysate (Total extract) and isolated EVs secreted by equal numbers of TvVPS32 or TvEpNEO were analyzed by immunoblotting to evaluate the upresence of three proteins previously detected in the exosome and MVs proteomes (TvTSP1, TvMIF and TvTCTP proteins). Same number of initial cells and same volume of sample was used for comparison. Hmp33 (a hydrogenosomal protein) was used as loading control. One representative experiment out of three is shown. **e** Nanoparticle tracking analysis of isolated VPS32-EVs and EpNEO-EVs samples. The concentration of particles detected in each sample is shown. Three independent set of samples were analyzed

increasing parasite adherence is observed when the cells are pre-incubated with EVs isolated from TvVPS32 (Fig. 4d). These results may suggest that the protein content and/or binding capacity from EVs isolated from TvEpNEO or TvVPS32 could be different.

To evaluate if the EVs isolated from TvVPS32 have a modified binding capacity or uptake by host cell, we labeled 10 µg of *T. vaginalis* EVs isolated from TvVPS32 and TvEpNEO with PKH67 dye and incubated with NHPrE1 prostate cells. After incubation and washing to remove unincorporated dye, host cells were then analyzed for PKH67 fluorescence using both microscopy and flow cytometry. As can be observed in the Fig. 5a and b, the fluorescence intensity analyzed by microscopy of NHPrE1 cells incubated with EVs isolated from TvVPS32 is ~35% higher than host cells incubated with EVs isolated from TvEpNEO parasites (Fig. 5a and b). To demonstrate that the binding is specific, fluorescently labeled PBS were also included as a control. In this case, minimal fluorescence was detected (Fig. 5a and b).

We also visualized the uptake of EVs using flow cytometer. Endocytosis is the primary pathway for EVs uptake and recently, it was demonstrated that *T. vaginalis* EVs uptake may be blocked at 4 °C [43]. Hence, to evaluate if the observed differences could be attributed to an effect

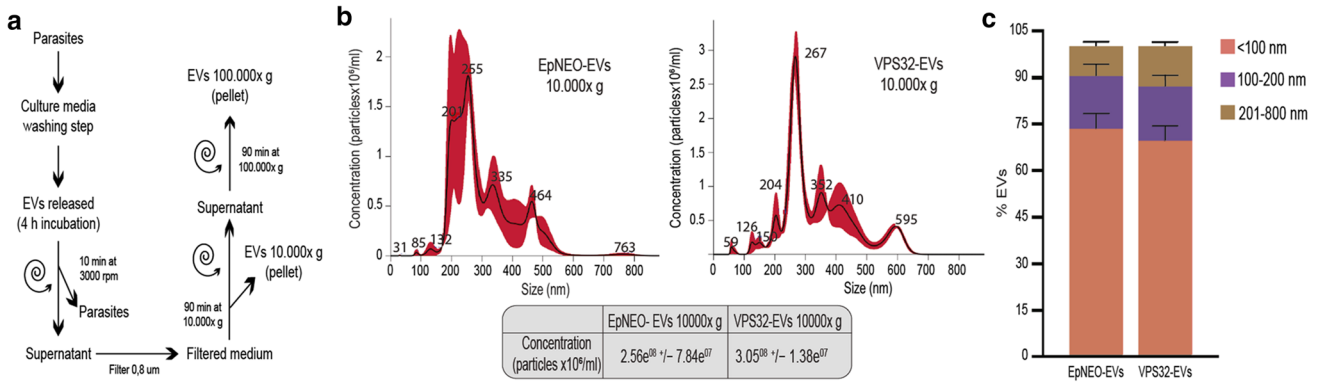

Fig. 3 **a** Differential EVs isolation protocol. **b** Concentration and size of EVs isolated at 10.000 × g from TvVPS32 and TvEpNEO control parasites analyzed by NTA. **c** Size of isolated EVs analyzed using negative staining EM. The diameter of 500 EVs was measured

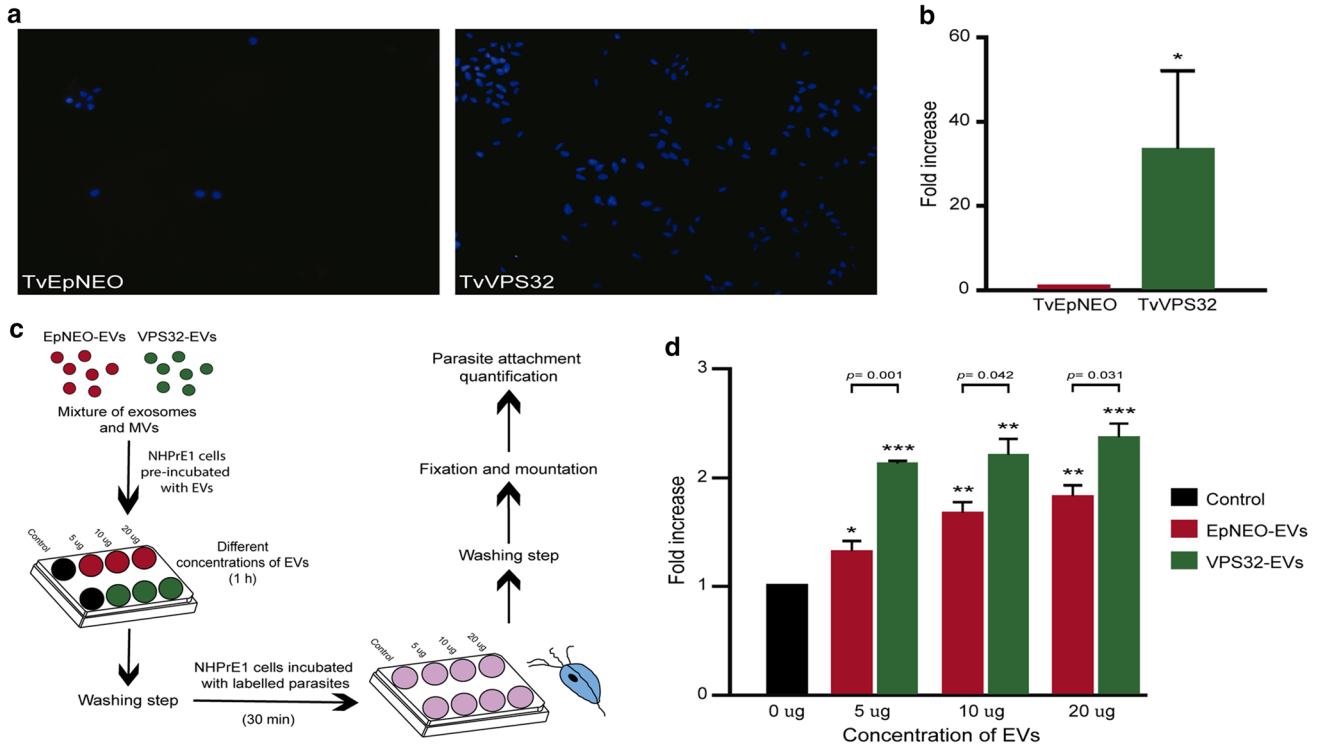

Fig. 4 Attachment of TvEpNEO and TvVPS32 parasites to NhPRE1 cells. **a** TvEpNEO and TvVPS32 parasites were labeled with Cell Tracker Blue CMAC (Invitrogen). Labeled parasites were then incubated for 30 min with NhPRE1 prostate cell monolayers grown on coverslips in 24-well plates at 37 °C and 5% CO2. Coverslips were washed to remove non-adherent parasites, mounted, and visualized by fluorescence microscopy. **b** Adherence of TvEpNEO (red bar) and TvVPS32 (green bar) parasites to NhPRE1 cells. Data are from three experiments performed in triplicate and show the fold increase in the number of parasites attached per coverslip standardized using TvEpNEO parasites with SD ($p < 0.05$). **c** Schematic representation of the experimental design. EVs from TvEpNEO (red) and TvVPS32 (green) were isolated. NhPRE1 cells were pre-incubated with increasing amount of EVs. Then, parasite attachment was analyzed by fluorescent microscopy. **d** Preincubation of NhPRE1 cells with VPS32-EVs or EpNEO-EVs increases adherence of a poorly adherent *T. vaginalis* strain (G3). Note that a stronger effect in increasing parasite adherence is observed when the cells are pre-incubated with EVs isolated from parasites transfected with VPS32. Statistical analyses were performed by comparing the adherence values of each treatment against the control treatment (*$p < 0.05$, **$p < 0.01$, ***$p < 0.001$). Besides, statistical analyses within each treatment were performed comparing between EVs concentration

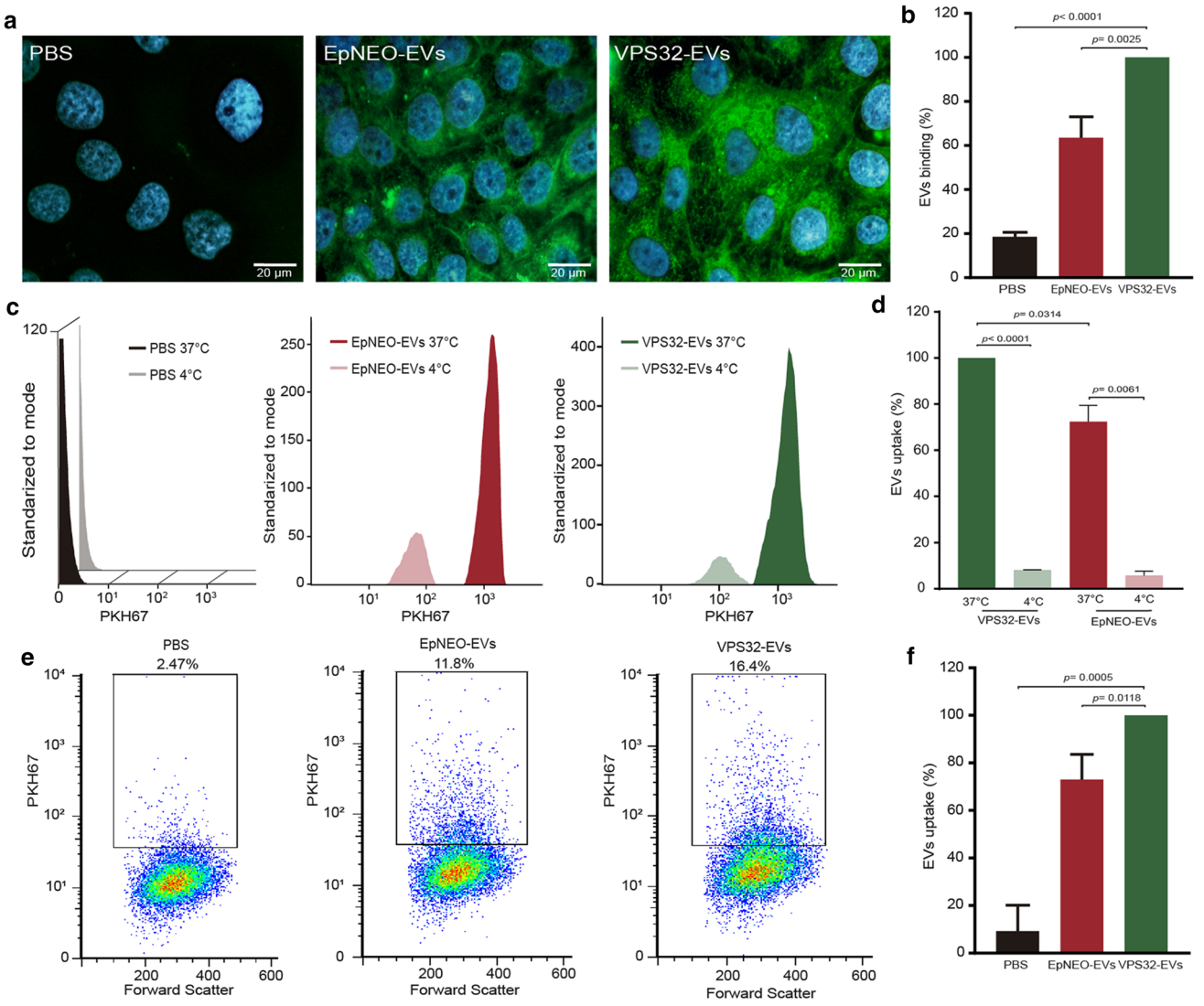

Fig. 5 Analysis of EVs uptake by prostate cells. **a** *T. vaginalis* VPS32-EVs or EpNEO-EVs were labeled with PKH67 dye and incubated with NhPRE1cells for 3 h. EV binding was visualized using fluorescence microscopy by incubating NhPRE1 cells with PKH67-labeled EVs or PKH67-labeled PBS as control (green). The nucleus was stained with DAPI (blue). The images are representative of 20 images viewed under similar conditions. **b** Quantification of EVs binding. Data shown represent the mean ± SD from 3 independent experiments, each performed in duplicate. The maximal fluorescence after incubating with labeled EVs was arbitrarily set at 100%. **c** Effect on uptake by temperature that block endocytosis of fluorescently labeled VPS32-EVs or EpNEO-EVs detected using flow cytometry. *T. vaginalis* VPS32-EVs or EpNEO-EVs were labeled with PKH67 dye, incubated with NhPRE1 cells at 37 °C or 4 °C for 45 min and uptake was quantified by flow cytometry. **d** Quantification of VPS32-EVs or EpNEO-EVs uptake at 37 °C or 4 °C. The maximal fluorescence after incubating with labeled VPS32-EVs was arbitrarily set at 100%. **e** *T. vaginalis* VPS32-EVs or EpNEO-EVs were labeled with PKH67 dye, incubated with NhPRE1cells for 45 min at 37 °C and the binding quantified using flow cytometry. Three independent experiments were performed. A representative experiment is shown. **f** Quantification of PKH67-labeled EVs uptake to NhPRE1 cells using flow cytometry. The maximal fluorescence after incubating the NhPRE1 cells with labeled VPS32-EVs was set at 100%. Data are presented are the mean ± SD from three independent experiments

in differential uptake by host cells, we performed an EV uptake inhibition experiment by incubating the labelled isolated EVs with NHPrE1 prostate cells at 37 °C and 4 °C (Fig. 5c and d). As can be observed, an inhibition in uptake at 4 °C is observed when NHPrE1 cells are incubated with EVs isolated from TvVPS32 or EpNEO parasites. Importanly, when the incubation is performed at 37 °C, the EV uptake is higher when the NHPrE1 cells are incubated with EVs isolated from TvVPS32. Similarly, 16,4% and 11,8% of PKH67 fluorescence was detected in host cells incubated with EVs isolated from TvVPS32 and TvEpNEO parasites, respectively, whereas only 2,17% of PKH67 fluorescence were observed in host cells incubated PKH67 labeled PBS (Fig. 5e and f).

To evaluate if TvVPS32 might be an EV ligand, we pre-incubated 10 µg of VPS32-EVs with different concentration of anti-HA antibody. Analysis by flow cytometry and fluorescence microscopy demonstrate that TvVPS32 is not an EV ligand critical for EV internalization as incubation with anti-HA does not affect the EVs uptake (Fig. 1S).

VPS32 regulates protein cargo sorting into EVs

Our results here indicate that TvVPS32 isolated EVs have higher binding to host cells capacity, suggesting that VPS32 might be affecting the EVs protein cargo sorting. To evaluate this, we attempted to gain insight into proteins contained in EVs isolated from TvVPS32 that may potentially point to a mechanism for the increased parasite adherence to host cells. To determine whether VPS32 might be regulating EVs protein cargo composition, a quantitative analysis using liquid chromatography-tandem mass spectrometry (LC–MS/MS) proteomic approach was performed on three biologically independent samples of equal amount of EVs isolated from TvEpNEO-control and TvVPS32-overexpressing parasites. Comparison of protein abundance was evaluated by LFQ intensities using the online-server LFQ-Analyst [44]. Proteins with two or more identified peptides that were found in at least two of three mass spectrometry set of samples were included in the EVs' proteome. After excluding contaminants, a total of 483 T. *vaginalis* proteins were identified in the EVs isolated from the TvEpNEO and TvVPS32 (see Table S1 in the Supplemental material). We further compared the obtained proteomic data with the previously published *T. vaginalis* exosomes [9] and MVs proteome [10] as well as with the surface proteome [45]. Although different parasite strains were used in those studies, we found that 314 out of 483 proteins detected in our proteome were also present in the previously published MVs, exosomes and/or surface proteomes [9, 10, 41] (Table S1 in the supplemental material), indicating that our samples contain EVs. To search for proteins that are over-represented in VPS32-EVs samples relative to EpNEO-EVs control, LFQ data was converted to $\log_2$ scale, samples were grouped by conditions and missing values were imputed using Deterministic Minimum Imputation (MinDet) [46]. Proteins that exhibited changes in LFQ intensities that were greater than twofold and possessed p values of less than 0.05 were considered differentially expressed. Using this approach, 36 proteins were determined to be differentially expressed between VPS32 and EpNEO-EVs, 29 of which were up-regulated by twofold or greater abundance in VPS32-EVs samples (Fig. 6a and Table 1). By contrast, 7 proteins were found to be less abundant in VPS32-EVs than in EpNEO-EVs by 2-fold or more (Fig. 6a and Table 1). These data support our previous conclusions that the EVs from TvVPS32 cells may be selectively loaded

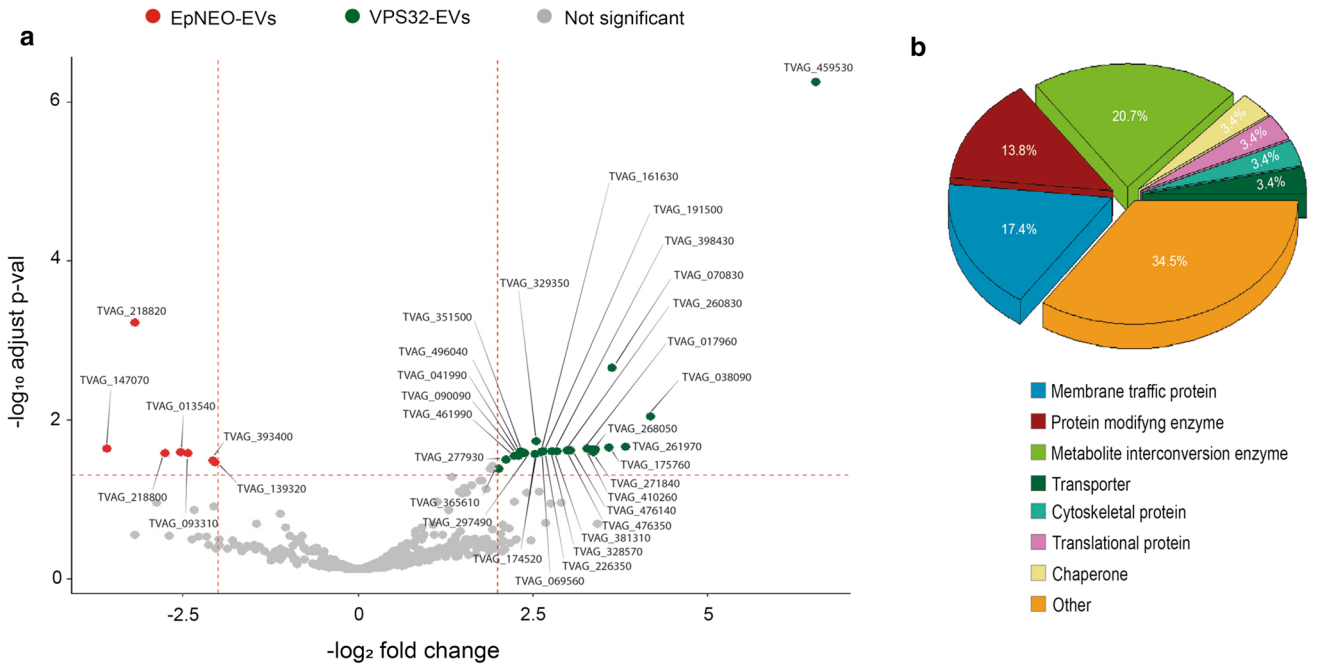

Fig. 6 EVs proteins identified by LC–MS/MS analysis. **a** A volcano plot of $-\log10$(p-value) versus $-\log_2$(fold change) depicting the 483 proteins identified in the EVs isolated from TvVPS32 and TvEpNEO was constructed. Data points to the right, colored green, denote proteins which exhibited fold changes of VPS32-EVs/EpNEO-EVs greater than 2 (29 proteins). Data points to the left, colored red, denote proteins which exhibited fold changes of EpNEO/VPS32 greater than 2 (7 proteins). **b** Proteins differentially detected in the EVs isolated from TvVPS32 were sorted into functional groups using genome annotation. Most representative groups are shown

Table 1 Differentially expressed EVs proteins identified by LC–MS/MS analysis

Locus	Protein names	Fold change
More abundant in VPS32 EVs		
TVAG_459530	VPS32 protein	42.90
TVAG_038090	Alkyl hydroperoxide reductase, subunit C	17.56
TVAG_261970; TVAG_420500; TVAG_420510	Carbamate kinase	14.67
TVAG_070830	Cytidylate kinase	13.18
TVAG_175760	Conserved hypothetical protein	12.89
TVAG_268050	Phosphoglycerate kinase	11.49
TVAG_017960	Conserved hypothetical protein	11.29
TVAG_271840	F-actin capping protein beta subunit	11.22
TVAG_410260	Clan CA, family C1, cathepsin L-like cysteine peptidase	10.69
TVAG_476140	Peptidylprolyl isomerase	9.24
TVAG_260830	Conserved hypothetical protein	9.12
TVAG_476350	Conserved hypothetical protein	8.94
TVAG_381310	Malate and lactate dehydrogenase	8.12
TVAG_328570	TRNA binding domain containing protein	7.78
TVAG_161630	Conserved hypothetical protein	7.67
TVAG_398430	C2 domain containing protein	7.67
TVAG_226350	Clathrin coat assembly protein ap-1	7.02
TVAG_069560	O-linked N-acetylglucosamine transferase, ogt	6.97
TVAG_191500	Clan MA, family M8, leishmanolysin-like protein	6.86
TVAG_329350; TVAG_355600; TVAG_456910	Rab5	6.50
TVAG_174520	Neuroendocrine differentiation factor	6.45
TVAG_496040	Conserved hypothetical protein	5.71
TVAG_351500	Rab7	5.43
TVAG_297490	Clathrin light chain	5.29
TVAG_461990; TVAG_162010; TVAG_607280; TVAG_530020	Leucine-rich repeat protein, BspA family	5.29
TVAG_041990	C2 domain containing protein	5.20
TVAG_090090	Clan MH, family M20, peptidase T-like metallopeptidase	4.97
TVAG_277930	Conserved hypothetical protein	4.49
TVAG_365610	Leucine-rich repeat protein, BspA family	4.08
More abundant in EpNEO EVs		
TVAG_147070	Chaperonin containing t-complex protein 1, delta subunit, tcpd	12.89
TVAG_218820	Conserved hypothetical protein	10.18
TVAG_218800	Conserved hypothetical protein	7.62
TVAG_013540	DNAj/HSP40	6.40
TVAG_093310	Brix domain containing protein	5.90
TVAG_393400	Conserved hypothetical protein	4.28
TVAG_139320; TVAG_151620	Heat shock protein	4.16

with specific groups of proteins that may be thus exerting specific functions. As expected, although VPS32 was recovered in the EVs isolated from both TvVPS32 and TvEpNEO, it was ~ 43-fold more abundant in EVs isolated from VPS32-overexpressing cells (Table 1). Interestingly, several proteins that function as key regulators of membrane trafficking, including two Rab proteins (Rab5; ~ 6-fold and Rab 7, ~ 5-fold) and two Clathrin-related proteins (Clathrin light chain, ~ 5-fold and AP-1 clathrin adaptor, ~ 7-fold), were found to be more abundant in EVs from TvVPS32 cells (Table 1). Other proteins of interest with similarity to known proteins that were significantly more abundant with the presence of VPS32 included three proteins with kinase activity (~ 14-, ~ 13- and ~ 11-fold) and metabolic enzymes (~ 8- and ~ 7-fold) (Fig. 5b).

Seven additional hypothetical proteins were found to be ~ 13-, 11-, ~ 9-, ~ 9-, ~ 7- and 6-fold more abundant on the EVs isolated from TvVPS32-overexpressing

parasites (Table 1). Of particular interest, several proteins that might be related to parasite pathogenesis were more abundant in EVs from TvVPS32-producing cells; including two members of the leucine-rich repeat BspA family proteins (~ 5- and ~ fourfold) and three peptidases (cathepsin L-like cysteine peptidase, ~ 11-fold; leishmanolysin-like protein, ~ 7-fold; and peptidase T-like metallopeptidase, ~ 5-fold); (Table 1). Collectively, these data indicate that EVs from VPS32-producing cells may contain a diverse set of unique or upregulated proteins that might be contributing, at least in part, to the observed effect in parasite adherence.

Discussion

The role of ESCRT proteins in EVs biogenesis has been widely studied in mammals [10, 31–33]. The ESCRT complex has been shown to direct the scission of vesicles that bud away from the cytosol, whether into internal compartments or out of the cell. Specifically, it has been proposed that the ESCRT III complex forms filaments, flat spirals, tubes and conical funnels, that are thought to somehow direct membrane remodeling and scission; key processes involved in the generation of intraluminal vesicles (ILVs) in endosomes and release MVs from the plasma membrane [47]. Although the ESCRT pathway is generally thought to be the main driver of EV biogenesis in mammalian cells, the function of these conserved proteins in unicellular eukaryotic pathogens is limited. Here, we have established a role for VPS32, a member of the ESCRT III complex, in biogenesis and protein cargo sorting into extracellular vesicles in the parasite *T. vaginalis*. In this sense, it has been recently described that the protozoan parasite *Giardia lamblia*, although lacking a classical endo-lysosomal pathway, is able to release exosome-like vesicles (ElV) depending on the ESCRT-associated AAA + -ATPase Vps4a, Rab11, and ceramide [25]. Similarly, gene silencing of the ESCRT factor Vps36, compromises exosome secretion in the parasite *Trypanosome brucei* [48].

The results obtained here not only demonstrated that VPS32 has a role in EV biogenesis, but that this protein also plays central role in regulation of parasite attachment to prostate cells. Importantly, the identification of ESCRT proteins as key players in regulation of pathogenesis in a unicellular eukaryote has never been proposed. While *T. vaginalis* attachment to host cells likely depends on multiple factors [41, 49–52], the increase in host binding observed upon VPS32 overexpression is the most striking phenotypic effect mediated by exogenous expression of a single protein factor. The strongest effect in host cell binding mediated by a single protein that had been previously observed was with Cadherin-like Protein (CLP), which increase parasite attachment by 3.5-fold when overexpressed [49]. Based on these antecedents and taken in consideration the drastic effect in parasite attachment upon overexpression of TvVPS32, it would be interesting to evaluate whether this protein mediate its function trough association with other proteins or molecules. Considering that previous works described an important role of EVs in modulating parasite attachment [9, 10], the observed phenotype of TvVPS32 transfected parasites in parasite adherence might be explained, at least partially, due to an increase in the release of EVs. In this sense, similar as previously described [9], we have confirmed here that EVs have a role in modulation of parasite:host cell binding as the pre-incubation of host cells with EVs isolated from TvVPS32-overexpressing or TvEpNEO increased the binding to host cells of a poorly adherent strain. It is interesting to note that a stronger effect in increasing parasite adherence is observed when the cells are pre-incubated with EVs isolated from TvVPS32. This observation might suggest that protein content from EVs isolated from TvEpNEO or TvVPS32 is different. Indeed, supported by the identification of 29 proteins that are > 2-fold more abundant in VPS32-EVs than in EpNEO-EVs (Table 1), quantitative proteomic analyses showed that EVs from TvVPS32-producing cells are enriched in specific cargo. Interestingly, we found that increased expression of VPS32 leads to a higher amount of clathrin and clathrin coat assembly AP1 as well as proteins with kinase activity in EVs. Vesicle budding and cargo selection at different stages of the exocytic and endocytic pathways are mediated by different coats and sorting signals. The coats deform flat membrane patches into round buds, eventually leading to the release of coated vesicles. Additionally, the coats are also involved in regulation of cargo selection through recognition of sorting signals present in the cytosolic domains of transmembrane cargo proteins [53]. Clathrin coats were initially assumed to participate in most of vesicular transport steps within the cell. Moreover, clathrin vesicle assembly is regulated by kinases, phosphatases, and other accessory proteins [54]. Cargo sorting and ILVs formation occurs by coordinated and repetitive recruitment waves of ESCRT subcomplexes, and recently, it has been reported that clathrin recruitment to endosomes is required for these normal ESCRT complex kinetics [55]. The fact that we were able to detect these proteins at elevated levels in EV preparations from TvVPS32-producing cells may indicate that this protein stimulates their production or sorting, potentially as direct or indirect targets of VPS32 regulation. Exosome release has also been facilitated by various mechanisms and harbor different cargos. Specifically, Rab4, Rab5, Rab11, Rab35, Rab27a and Rab27b proteins have been implicated in different steps of exosome release in different cell types [56]. Additionally, Rab7 appears to contribute to shedding vesicles release from the tip of primary cilium [57]. In concordance, we detected larger amounts of

Rab5 and Rab7 in the proteomic analyses of EV preparations from TvVPS32-producing cells, which could suggest a role of these proteins in extracellular vesicles biogenesis or release in this parasite. However, further studies are needed to establish the specific function of Rab proteins within this process in trichomonads.

Moreover, some proteins previously associated to *T. vaginalis* pathogenesis have been identified as differentially expressed. Specifically, two members of the cell surface BspA protein family may be concentrated within EVs from TvVPS32 cells. In bacteria, the BspA proteins have a role in the colonization of the oral mucosa and triggering of the host immune response [58]. Importantly, a synergistic effect of BspA and outer membrane vesicles (OMVs) related to adherence and colonization epithelial cells has also been demonstrated [59]. In *Entamoeba histolytica,* reduced levels of a BspA family protein block parasite invasion to the human colon mucosal and a BspA-like protein (EHI_016490) seems to function as a chemoattractant receptor for tumor necrosis factor [60]. More importantly, some authors suggested that *T. vaginalis* BspA proteins might have a similar function to bacteria as the over-expression of a BspA protein (TVAG_240680) increased the adhesion to VECs in a poorly adherent *T. vaginalis* strain [61]. Although further studies are needed to understand the role of this protein family within EVs, the presence of two BspA proteins in the EV proteome of TvVPS32 parasites might indicate that they could potentially play a role in the binding of EVs to host cells. A malate dehydrogenase protein was also detected in higher amount in VPS32-EVs. Interestingly, it has been previously described that malate dehydrogenase is present in large amounts in amoeboid trophozoites of *T. vaginalis* bound to fibronectin [62]. Moreover, some malate dehydrogenase isoforms were differentially expressed in a highly virulence fresh clinical isolate of *T. vaginalis* [63]. These results might be indicating a role of this protein in adherence of the parasite to the host cells. Furthermore, an assortment of upregulated peptidases including a cathepsin L-like cysteine peptidase, a Clan MA, family M8, leishmanolysin-like protein (or GP63) and a M20 metallopeptidase, was also seen in VPS32-EVs. It is known that *T. vaginalis* produces several types of proteases such as serine proteases, cysteine proteases, and metalloproteinases, that are proposed as important regulators of invasion and pathogenesis [64, 65]. In strong support of this, the presence of numerous trichomonad proteinases has been detected in vaginal washes of infected women [66]. As *T. vaginalis* extracellular cysteine peptidases have a role in the degradation of the mucin layer that covers epithelial cells [67], it is possible that the presence of proteases in vaginal washes of infected women may play a role in degrading host proteins or extracellular matrix to clear the attachment site [68]. In this sense, GP63 proteases are important virulence factor that contribute to *Leishmania* survival during the initial moment of the infection that are present in the exosome proteome [69]. In *T. vaginalis*, 48 members of the GP63 protease family has been identified [70]. Although the role of these metalloproteinases has not been fully elucidated, it has been proposed that they play a vital role in the infection process [65]. Finally, 7 out of 29 proteins differentially expressed are hypothetical proteins that are unique to *T. vaginalis*. The ability to identify these novel EVs proteins provides a foundation for future studies with the potential of uncovering unpredicted host-parasite interactions that may be important for pathogenesis. It has been previously suggested that differential expression of specific protein families might modulate parasite adherence [41, 71]. In this sense, previous reports showed that pre-incubation of host cells with EVs isolated from highly adherent *T. vaginalis* strains induce a strong affect in host cell binding, whereas exosomes isolated from less adherent strains have only a minor effect on binding; indicating that EVs contain strain-specific factors responsible for the differential binding phenotype [9]. Our results put forward this idea and suggest that, depending on the cargoes associated with different EVs populations, the parasite attachment to host cells may be affected. The contents of EVs appear to be highly selective and the ESCRT-III complex might be a key regulator to enrich for specific cargoes. It will be important in the future to elucidate the molecular requirements for these different EVs cargoes within the different strains that might be affecting the parasite adherence to host cells.

These observations will certainly contribute to our understanding on the molecular mechanisms involved in vesicular cargo-sorting and biogenesis. In the future, continuing improvements of CRISPR-mediated genome editing approaches will enable us to modulate the nature of EVs and their composition to gain a better understanding of the dynamic actions of the ESCRT machinery in regulation of EVs biogenesis and parasite pathogenesis.

Supplementary Information The online version contains supplementary material available at https://doi.org/10.1007/s00018-021-04083-3.

Acknowledgements We thank our colleagues in the lab for helpful discussions. This research was supported with a Grant from the Agencia Nacional de Promoción Científica y Tecnológica (ANPCyT) Grant BID PICT-2019-01671 (NdM). NdM and VMC are researchers from the National Council of Research (CONICET) and UNSAM. NS is a PhD fellow from CONICET. The funders had no role in study design, data collection and analysis, decision to publish, or preparation of the manuscript.

Funding This research was supported with a Grant from the Agencia Nacional de Promoción Científica y Tecnológica (ANPCyT) Grant BID PICT-2019-01671 (NdM).

Availability of data and material Data are provided as a supplementary table.

Code availability Not applicable.

Declarations

Conflict of interest The authors declare that no competing interests exist.

References

1. WHO (2018) Report on global sexually transmitted infection surveillance. pp 63
2. Fichorova RN (2009) Impact of *T. vaginalis* infection on innate immune responses and reproductive outcome. J Reprod Immunol 83:185–189. https://doi.org/10.1016/j.jri.2009.08.007
3. Van Der Pol B, Kwok C, Pierre-Louis B et al (2008) Trichomonas vaginalis infection and human immunodeficiency virus acquisition in African women. J Infect Dis 197:548–554. https://doi.org/10.1086/526496
4. McClelland RS, Sangaré L, Hassan WM et al (2007) Infection with *Trichomonas vaginalis* increases the risk of HIV-1 acquisition. J Infect Dis 195:698–702. https://doi.org/10.1086/511278
5. Twu O, Dessi D, Vu A et al (2014) Trichomonas vaginalis homolog of macrophage migration inhibitory factor induces prostate cell growth, invasiveness, and inflammatory responses. Proc Natl Acad Sci USA 111:8179–8184. https://doi.org/10.1073/pnas.1321884111
6. Gander S, Scholten V, Osswald I et al (2009) Cervical dysplasia and associated risk factors in a juvenile detainee population. J Pediatr Adolesc Gynecol 22:351–355. https://doi.org/10.1016/j.jpag.2009.01.070
7. Mercer F, Johnson PJ (2018) *Trichomonas vaginalis*: pathogenesis, symbiont interactions, and host cell immune responses. Trends Parasitol 34:683–693. https://doi.org/10.1016/j.pt.2018.05.006
8. Nievas YR, Lizarraga A, Salas N et al (2020) Extracellular vesicles released by anaerobic protozoan parasites: current situation. Cell Microbiol 22:e13257. https://doi.org/10.1111/cmi.13257
9. Twu O, de Miguel N, Lustig G et al (2013) Trichomonas vaginalis exosomes deliver cargo to host cells and mediate hostratioparasite interactions. PLoS Pathog 9:e1003482. https://doi.org/10.1371/journal.ppat.1003482
10. Nievas YR, Coceres VM, Midlej V et al (2018) Membrane-shed vesicles from the parasite *Trichomonas vaginalis*: characterization and their association with cell interaction. Cell Mol Life Sci 75:2211–2226. https://doi.org/10.1007/s00018-017-2726-3
11. van Niel G, D'Angelo G, Raposo G (2018) Shedding light on the cell biology of extracellular vesicles. Nat Rev Mol Cell Biol 19:213–228. https://doi.org/10.1038/nrm.2017.125
12. Andreu Z, Yáñez-Mó M (2014) Tetraspanins in extracellular vesicle formation and function. Front Immunol 5:442. https://doi.org/10.3389/fimmu.2014.00442
13. Colombo M, Raposo G, Thery C (2014) Biogenesis, secretion, and intercellular interactions of exosomes and other extracellular vesicles. Annu Rev Cell Dev Biol 30:255–289. https://doi.org/10.1146/annurev-cellbio-101512-122326
14. Henne WM, Buchkovich NJ, Emr SD (2011) The ESCRT pathway. Dev Cell 21:77–91. https://doi.org/10.1016/j.devcel.2011.05.015
15. Roxrud I, Stenmark H, Malerød L (2010) ESCRT & Co. Biol Cell 102:293–318. https://doi.org/10.1042/bc20090161
16. Cocucci E, Meldolesi J (2015) Ectosomes and exosomes: shedding the confusion between extracellular vesicles. Trends Cell Biol 25:364–372. https://doi.org/10.1016/j.tcb.2015.01.004
17. Schmidt O, Teis D (2012) The ESCRT machinery. Curr Biol CB 22:R116–R120. https://doi.org/10.1016/j.cub.2012.01.028
18. Fang Y, Wu N, Gan X et al (2007) Higher-order oligomerization targets plasma membrane proteins and HIV gag to exosomes. PLoS Biol 5:e158–e158. https://doi.org/10.1371/journal.pbio.0050158
19. Van Engelenburg SB, Shtengel G, Sengupta P et al (2014) Distribution of ESCRT machinery at HIV assembly sites reveals virus scaffolding of ESCRT subunits. Science 343:653–656. https://doi.org/10.1126/science.1247786
20. Bissig C, Gruenberg J (2014) ALIX and the multivesicular endosome: ALIX in Wonderland. Trends Cell Biol 24:19–25. https://doi.org/10.1016/j.tcb.2013.10.009
21. Nabhan JF, Hu R, Oh RS et al (2012) Formation and release of arrestin domain-containing protein 1-mediated microvesicles (ARMMs) at plasma membrane by recruitment of TSG101 protein. Proc Natl Acad Sci U A 109:4146–4151. https://doi.org/10.1073/pnas.1200448109
22. Saksena S, Wahlman J, Teis D et al (2009) Functional reconstitution of ESCRT-III assembly and disassembly. Cell 136:97–109. https://doi.org/10.1016/j.cell.2008.11.013
23. Lenz M, Crow DJG, Joanny J-F (2009) Membrane buckling induced by curved filaments. Phys Rev Lett 103:38101. https://doi.org/10.1103/PhysRevLett.103.038101
24. Fabrikant G, Lata S, Riches JD et al (2009) Computational model of membrane fission catalyzed by ESCRT-III. PLoS Comput Biol 5:e1000575. https://doi.org/10.1371/journal.pcbi.1000575
25. Moyano S, Musso J, Feliziani C et al (2019) Exosome biogenesis in the protozoa parasite giardia lamblia: a model of reduced interorganellar crosstalk. Cells. https://doi.org/10.3390/cells8121600
26. Iriarte LS, Midlej V, Frontera LS et al (2018) TfVPS32 regulates cell division in the parasite *Tritrichomonas foetus*. J Eukaryot Microbiol 65:28–37. https://doi.org/10.1111/jeu.12424
27. Clark CG, Diamond LS (2002) Methods for cultivation of luminal parasitic protists of clinical importance. Clin Microbiol Rev 15:329–341. https://doi.org/10.1128/cmr.15.3.329-341.2002
28. Jiang M, Strand DW, Fernandez S et al (2010) Functional remodeling of benign human prostatic tissues in vivo by spontaneously immortalized progenitor and intermediate cells. Stem Cells 28:344–356. https://doi.org/10.1002/stem.284
29. Delgadillo MG, Liston DR, Niazi K, Johnson PJ (1997) Transient and selectable transformation of the parasitic protist *Trichomonas vaginalis*. Proc Natl Acad Sci USA 94:4716–4720. https://doi.org/10.1073/pnas.94.9.4716
30. Théry C, Witwer KW, Aikawa E et al (2018) Minimal information for studies of extracellular vesicles 2018 (MISEV2018): a position statement of the international society for extracellular vesicles and update of the MISEV2014 guidelines. J Extracell Vesicles 7:1535750. https://doi.org/10.1080/20013078.2018.1535750
31. Florens L, Carozza MJ, Swanson SK et al (2006) Analyzing chromatin remodeling complexes using shotgun proteomics and normalized spectral abundance factors. Methods San Diego Calif 40:303–311. https://doi.org/10.1016/j.ymeth.2006.07.028
32. Kaiser P, Wohlschlegel J (2005) Identification of ubiquitination sites and determination of ubiquitin-chain architectures by mass spectrometry. Methods in enzymology. Academic Press, Cambridge, pp 266–277
33. Wohlschlegel JA (2009) Identification of SUMO-conjugated proteins and their SUMO attachment sites using proteomic mass spectrometry. Methods Mol Biol Clifton NJ 497:33–49. https://doi.org/10.1007/978-1-59745-566-4_3
34. Kelstrup CD, Young C, Lavallee R et al (2012) Optimized fast and sensitive acquisition methods for shotgun proteomics on a quadrupole orbitrap mass spectrometer. J Proteome Res 11:3487–3497. https://doi.org/10.1021/pr3000249

35. Tyanova S, Temu T, Cox J (2016) The MaxQuant computational platform for mass spectrometry-based shotgun proteomics. Nat Protoc 11:2301–2319. https://doi.org/10.1038/nprot.2016.136
36. Aurrecoechea C, Brestelli J, Brunk BP et al (2009) GiardiaDB and TrichDB: integrated genomic resources for the eukaryotic protist pathogens *Giardia lamblia* and *Trichomonas vaginalis*. Nucleic Acids Res 37:D526–D530. https://doi.org/10.1093/nar/gkn631
37. Cociorva D, Tabb DL, Yates JR (2006) Validation of tandem mass spectrometry database search results using DTASelect. Curr Protoc Bioinform 16:13.4.1-13.4.14. https://doi.org/10.1002/0471250953.bi1304s16
38. Elias JE, Gygi SP (2007) Target-decoy search strategy for increased confidence in large-scale protein identifications by mass spectrometry. Nat Methods 4:207–214. https://doi.org/10.1038/nmeth1019
39. Tabb DL, McDonald WH, Yates JR 3rd (2002) DTASelect and contrast: tools for assembling and comparing protein identifications from shotgun proteomics. J Proteom Res 1:21–26. https://doi.org/10.1021/pr015504q
40. Mi H, Muruganujan A, Thomas PD (2013) PANTHER in 2013: modeling the evolution of gene function, and other gene attributes, in the context of phylogenetic trees. Nucleic Acids Res 41:D377-386. https://doi.org/10.1093/nar/gks1118
41. de Miguel N, Lustig G, Twu O et al (2010) Proteome analysis of the surface of Trichomonas vaginalis reveals novel proteins and strain-dependent differential expression. Mol Cell Proteom 9:1554–1566. https://doi.org/10.1074/mcp.M000022-MCP201
42. dos Santos O, de Vargas RG, Frasson AP et al (2015) Optimal reference genes for gene expression normalization in *Trichomonas vaginalis*. PLoS One 10:e0138331. https://doi.org/10.1371/journal.pone.0138331
43. Rai AK, Johnson PJ (2019) Trichomonas vaginalis extracellular vesicles are internalized by host cells using proteoglycans and caveolin-dependent endocytosis. Proc Natl Acad Sci 116:21354. https://doi.org/10.1073/pnas.1912356116
44. Shah AD, Goode RJA, Huang C et al (2020) LFQ-analyst: an easy-to-use interactive web platform to analyze and visualize label-free proteomics data preprocessed with MaxQuant. J Proteome Res 19:204–211. https://doi.org/10.1021/acs.jproteome.9b00496
45. Molgora BM, Rai AK, Sweredoski MJ et al (2021) A novel trichomonas vaginalis surface protein modulates parasite attachment via protein: host cell proteoglycan interaction. MBio. https://doi.org/10.1128/mBio.03374-20
46. Lazar C, Gatto L, Ferro M et al (2016) Accounting for the multiple natures of missing values in label-free quantitative proteomics data sets to compare imputation strategies. J Proteome Res 15:1116–1125. https://doi.org/10.1021/acs.jproteome.5b00981
47. Schöneberg J, Lee I-H, Iwasa JH, Hurley JH (2017) Reverse-topology membrane scission by the ESCRT proteins. Nat Rev Mol Cell Biol 18:5–17. https://doi.org/10.1038/nrm.2016.121
48. Eliaz D, Kannan S, Shaked H et al (2017) Exosome secretion affects social motility in *Trypanosoma brucei*. PLOS Pathog 13:e1006245. https://doi.org/10.1371/journal.ppat.1006245
49. Chen YP, Riestra AM, Rai AK, Johnson PJ (2019) A novel cadherin-like protein mediates adherence to and killing of host cells by the parasite *Trichomonas vaginalis*. MBio. https://doi.org/10.1128/mBio.00720-19
50. Riestra AM, Gandhi S, Sweredoski MJ et al (2015) A *Trichomonas vaginalis* rhomboid protease and its substrate modulate parasite attachment and cytolysis of host cells. PLoS Pathog 11:e1005294. https://doi.org/10.1371/journal.ppat.1005294
51. Bastida-Corcuera FD, Okumura CY, Colocoussi A, Johnson PJ (2005) Trichomonas vaginalis lipophosphoglycan mutants have reduced adherence and cytotoxicity to human ectocervical cells. Eukaryot Cell 4:1951–1958. https://doi.org/10.1128/ec.4.11.1951-1958.2005
52. Rendon-Gandarilla FJ, Ramon-Luing Lde L, Ortega-Lopez J et al (2013) The TvLEGU-1, a legumain-like cysteine proteinase, plays a key role in Trichomonas vaginalis cytoadherence. Biomed Res Int 2013:561979. https://doi.org/10.1155/2013/561979
53. Bonifacino JS, Glick BS (2004) The mechanisms of vesicle budding and fusion. Cell 116:153–166. https://doi.org/10.1016/s0092-8674(03)01079-1
54. Lafer EM (2002) Clathrin-protein interactions. Traffic Cph Den 3:513–520. https://doi.org/10.1034/j.1600-0854.2002.30801.x
55. Wenzel EM, Schultz SW, Schink KO et al (2018) Concerted ESCRT and clathrin recruitment waves define the timing and morphology of intraluminal vesicle formation. Nat Commun 9:2932. https://doi.org/10.1038/s41467-018-05345-8
56. Abels ER, Breakefield XO (2016) Introduction to extracellular vesicles: biogenesis, RNA cargo selection, content, release, and uptake. Cell Mol Neurobiol 36:301–312. https://doi.org/10.1007/s10571-016-0366-z
57. Wang G, Hu H-B, Chang Y et al (2019) Rab7 regulates primary cilia disassembly through cilia excision. J Cell Biol 218:4030–4041. https://doi.org/10.1083/jcb.201811136
58. Noël CJ, Diaz N, Sicheritz-Ponten T et al (2010) Trichomonas vaginalis vast BspA-like gene family: evidence for functional diversity from structural organisation and transcriptomics. BMC Genomics 11:99. https://doi.org/10.1186/1471-2164-11-99
59. Satoru I, Shinsuke O, Kuramitsu HK, Ashu S (2006) Porphyromonas gingivalis vesicles enhance attachment, and the leucine-rich repeat BspA protein is required for invasion of epithelial cells by "Tannerella forsythia." Infect Immun 74:5023–5028. https://doi.org/10.1128/IAI.00062-06
60. Silvestre A, Plaze A, Berthon P et al (2015) In Entamoeba histolytica, a BspA family protein is required for chemotaxis toward tumour necrosis factor. Microb Cell Graz Austria 2:235–246. https://doi.org/10.15698/mic2015.07.214
61. Handrich MR, Garg SG, Sommerville EW et al (2019) Characterization of the BspA and Pmp protein family of trichomonads. Parasit Vectors 12:406. https://doi.org/10.1186/s13071-019-3660-z
62. Huang K-Y, Huang P-J, Ku F-M et al (2012) Comparative transcriptomic and proteomic analyses of *Trichomonas vaginalis* following adherence to fibronectin. Infect Immun 80:3900–3911. https://doi.org/10.1128/IAI.00611-12
63. Cuervo P, Cupolillo E, Britto C et al (2008) Differential soluble protein expression between *Trichomonas vaginalis* isolates exhibiting low and high virulence phenotypes. J Proteomics 71:109–122. https://doi.org/10.1016/j.jprot.2008.01.010
64. Arroyo R, Alderete JF (1989) Trichomonas vaginalis surface proteinase activity is necessary for parasite adherence to epithelial cells. Infect Immun 57:2991–2997. https://doi.org/10.1128/iai.57.10.2991-2997.1989
65. Ma L, Meng Q, Cheng W et al (2011) Involvement of the GP63 protease in infection of *Trichomonas vaginalis*. Parasitol Res 109:71–79. https://doi.org/10.1007/s00436-010-2222-2
66. Alderete JF, Newton E, Dennis C, Neale KA (1991) The vagina of women infected with Trichomonas vaginalis has numerous proteinases and antibody to trichomonad proteinases. Genitourin Med 67:469–474. https://doi.org/10.1136/sti.67.6.469
67. Lehker MW, Sweeney D (1999) Trichomonad invasion of the mucous layer requires adhesins, mucinases, and motility. Sex Transm Infect 75:231. https://doi.org/10.1136/sti.75.4.231
68. Ryan CM, de Miguel N, Johnson PJ (2011) Trichomonas vaginalis: current understanding of host–parasite interactions. Essays Biochem 51:161–175. https://doi.org/10.1042/bse0510161
69. Olivier M, Atayde VD, Isnard A et al (2012) Leishmania virulence factors: focus on the metalloprotease GP63. Spec Issue Virulence

Factors Parasites 14:1377–1389. https://doi.org/10.1016/j.micinf.2012.05.014
70. Quan J-H, Choi I-W, Yang J-B et al (2014) Trichomonas vaginalis metalloproteinase induces mTOR cleavage of SiHa cells. Korean J Parasitol 52:595–603. https://doi.org/10.3347/kjp.2014.52.6.595
71. Pachano T, Nievas YR, Lizarraga A et al (2017) Epigenetics regulates transcription and pathogenesis in the parasite *Trichomonas vaginalis*. Cell Microbiol 19:e12716. https://doi.org/10.1111/cmi.12716